Semiconductor Physics, Quantum Electronics & Optoelectronics. 2003. V. 6, N 2. P. 254-258.

PACS: 42.25.-p, 42.25.-Hz, 42.87.Bg

Detection and metrology of optical vortex helical wave fronts

G.V. Bogatiryova, M.S. Soskin
Institute of Physics, NAS of Ukraine, 46 prospect Nauky, 03028 Kiev, Ukraine
E-mail: bogatyr@iop.kiev.ua

Abstract. Spatial structure of optical vortex helical wave fronts is for the first time directly tested using various interference arrangements and precise measuring techniques. Experimental data are compared with simulation results. On this base, advantages of interference technique of any kind for testing of optical vortices in solving the specific problems are revealed.

Keywords: singularity, optical vortex, helical wave front.

Paper received 20.01.03; accepted for publication 16.06.03.

1. Introduction

Singular optics dealing with the light fields possessing wave front dislocations grows rapidly in last decades [1-3], being the most fundamental branch of modern optics. It studies the fields bearing amplitude zeroes and phase jumps by π at some points or lines, or surfaces. There are resonator eigenmodes, i.e. transversal Hermite-Gaussian and Laguerre-Gaussian (LG) modes, Bessel beams, as well as waveguide modes; combined "smooth" and singular beams, speckle-fields; singular beams transformed by any optical system; diffraction patterns from screens and gratings, as well as fields in the vicinity of foci and caustics [3-6]. By analogy with defect crystalline structures, a phase jump of the field along any line perpendicular to the direction of propagation of the beam is referred to as the *edge dislocation*, while a phase change by $m2\pi$ ($m = 1,2,3...$) under circumference of the point of zero amplitude is referred to as the *screw dislocation* [1]. In the last case, a wave front is helical, and optical vortex (OV) is attributed by topological charge ($\pm m$) and orbital angular momentum [6].

Experimental singular optics develops since 1981 [5]. Theoretical predictions on vanishing of the field amplitude at singular point at transverse cross-section of a beam or along OV axis, where a phase becomes undeterminate and wave front acquires helical structure, have been qualitatively verified by the vast majority of experiments. Until now, however, these statements no underwent quantitative experimental verification. A notable exception is the paper [7], where advance precise technique is applied to test the edge dislocations produced by a relief diffraction grating. It has been shown that intensity of a field at singular point, actually, exceeds negligibly noise of a detector, and the phase jump on π occurs within the minimal resolved interval 10 nm.

Direct detecting of strictly zero magnitude of the field intensity at singular point is impossible due to finiteness of an area of the minimal receiving cell (pixel), noise of detector, and light scattering. In contrast, interference testing of helical structure of a wave front of OV at transverse cross-section (2D) had been performed yet in initial experiments on singular optics [8-10]. For that, spatial (3D) structure of a phase helicoid was not experimentally studied up to now. This problem is the subject of our communication. Section 2 is devoted to concise description of the structure of OVs, as well as the technique for producing of vortex beams by the use of a computer-generated hologram (CGH). We also represent computed interference patterns. In Section 3 we describe experimental procedure and results, including coaxial and off-axis interference of the modes LG_0^1 and LG_0^2 with divergent Gaussian beam kind of LG_0^0 – mode for controlled changes of optical path difference (OPD) among interfering beams. Experimental results are compared with computed ones. Advantages of any of interference techniques in solving of specific problems of singular optics are discussed in Section 4.

2. Structure, generation and detecting of optical vortices

The structure of LG mode is described in cylindrical coordinates ρ, φ, z by the expression [4]

$$E(LG_p^l) = E_0 \frac{w_0}{w(z)} \left(\frac{\sqrt{2}p}{w(z)} \right)^{|l|} \times$$
$$\times \exp\left(-\frac{\rho^2}{w(z)^2} \right) L_p^{|l|}\left(\frac{2\rho^2}{w(z)^2} \right) \times$$
$$\times \exp\left[i\left(\frac{k\rho^2}{2R(z)} + l\varphi - (2p + |l| + 1) \arctan\left(\frac{z}{z_R} \right) \right) \right],$$

where $p = 0,1,2,3,...$; $l = 0,\pm1,\pm2...$ are radial and azimuthal indices, respectively. Radial index characterizes the number of nodes of the field amplitude along the radius. When $l = 0$ or $|l| \neq 0$, the number of nodes is equal to p, or to $p + 1$, respectively. Modulus of azimutal index characterizes the number of wavelengths per helicoid pitch. w_0, $w(z)$ are radii of caustics ($z = 0$) and the beam at the distance z from caustics estimated by the level e^{-1} in respect of the maximal magnitude of amplitude; $k = 2\pi/\lambda$ is a wave number; z_R is the Raileigh distance; $R(z)$ is the radius of curvature of a wave front at the observation plane z. $L_p^{|l|}(x)$ are Laguerre polynomials [4]; in part, for $p = 0$ and 1, $L_0^{|l|}(x) = 1$ and $L_1^{|l|}(x) = |l| + 1 - x$, respectively. Magnitude of the topological charge of LG mode is determined as $m = l$. The sign of a charge is conventionally determined as "plus" or "minus" for right and left twirling of helical phase surface of the OV, respectively [3].

Amplitude distribution over the beam cross-section may be determined experimentally by photometric measuring of intensity distribution, while the phase related parameters of optical beam, such as radius of curvature and spatial form of a wave front, are measured interferentionally. As the parameters of a reference wave, such as amplitude distribution and radius of curvature of the wave front, are known, then coaxial interference pattern contains the data both on phase difference of the reference and tested beams at the each point of the observation plane (equiphase lines with the period $\Delta\phi = 2\pi$), and on difference of radii of curvature of the wave fronts (the number of interference fringes per unit area).

As it is well known [11], coaxial interference of two smooth wave fronts with different radii of curvature results in Fresnel rings. Gradual changing of OPD between two beams within λ manifests itself as running out of the rings from the center (or running them to the center), where bright fringe sare altered by dark ones and *vice versa*. In contrast, as one of two co-axially interfeing beams possesses helical wave front (as in the case of longitudinal OV), then the loci of constant phase difference of such a beam and reference beam with smooth wave front is spiral. The number of interference fringes nucleating at the center of spiral and the direction of twirling determine unambiguously the magnitude of the OV charge and its sign [3,10], see Fig. 1. So, if $R_S/R_{ref} > 1$ (R_S and R_{ref} are the radii of curvature of the singular beam and reference one, respectively), then left twirling corresponds to the negative charge, and the number of interference fringes nucleating at the OV core (one-star or two-star) is associated with modulus of the charge. Gradual changing of an OPD between two beams within λ manifests itself as intertwine or untwisting of a spiral. Thus, one can "scan" 3D helical phase surface interferentionally.

If the set of OVs exists at the field (for example, dipole of OVs or OVs at speckle field), coaxial interference pattern may be obtained for any one OV alone. Moreover, this pattern occurs to be distorted due to the presence of neighbouring OVs. On this reason, one applies off-axis interference technique for testing of such vortex bearing fields [5]. Each singular point just causes discontinuities of interference fringes with appearance of m additional fringes (so-called "forklets"). Magnitude of OV charge is determined directly by the number of such additional fringes at the forklet, and the sign of a charge is determined from known direction of propagation of a plane reference wave in respect to the singular beam [10], as it is shown in Fig. 2. Gradual changing of a phase difference between two beams within $m2\pi$ manifests itself as transformation of a forklet. So, additional bright interference fringes are bent and then turn into dark ones, but the position of fringe discontinuity remains un-

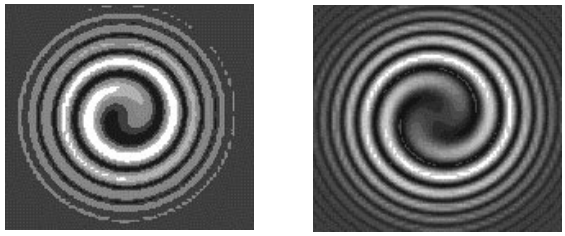

a *b*

Fig. 1. Computed structures resulting from coaxial interference of the spherical reference wave with singular beams of the charges $m = -1$ (*a*) and $m = -2$ (*b*); R_S/R_{ref}; OPD is $\Delta z = m\lambda$.

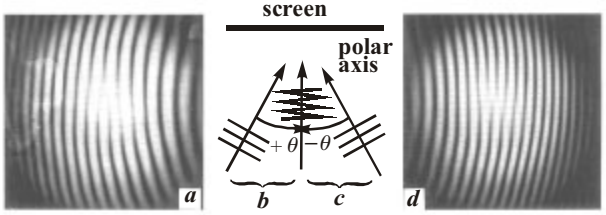

Fig. 2 [10]. Off-axis interferograms (*a*, *d*) of a wave front with a unity-charged screw dislocation ($m = 1$), and the corresponding interference schemes (*b*, *c*). A wave with screw dislocation propagates normally to the screen, the reference plane wave is tilted by an angle $\pm\theta$. Interferogram (*a*) corresponds to the orientation (*c*), where the reference wave-vector projection on the polar axis is negative, and the "forklet" is directed downwards.

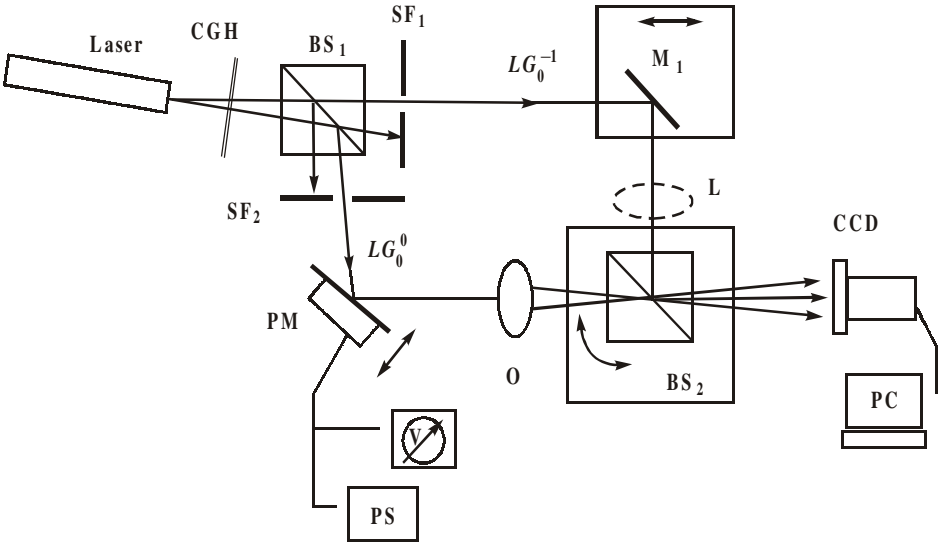

Fig. 3. Experimental arrangement for direct measurement of OV phase helical structure. CGH – computer generated hologram for reconstruction of Laguerre-Gaussian modes LG_0^{-1} and LG_0^{-2} at the minus-first and the minus-second orders, respectively; BS_1, BS_2 – beam-splitters; SF_1, SF_2 – spatial filters; M_1 – moving mirror; PM – piezoceramics-mounted mirror fed to the voltmeter V and the source of direct current PS; L – lens, O – objective.

changed. Comparison of computed and experimental results demonstrating transformations of off-axis interference pattern in the vicinity of OV with $m = -1$ will be presented in the following section (see Fig. 7).

3. Experiment and discussion

It has been proposed in Refs. [8,9,13] to generate LG modes with desirable p and l using a CGH, whose amplitude transmittance is calculated as an interference pattern from LG_0^1 – mode and Gaussian beam with a plane wave front at the plane of caustic. Spacing of a pattern is chosen in such a manner that the angle at the 1st diffraction order occurs to be in excess of angular divergence of laser beam enough to provide separation of the diffraction orders at desirable distance behind a CGH. CGH is prepared at amplitude photographic film that undergoes bleaching.

CGH is placed at the plane of caustics of unexpanded laser beam with diameter $2w_0 = 1.6$ mm, for which it was calculated. Diffraction of laser beam at phase grating results into reconstruction of $LG_0^{\pm n}$ – modes at nth orders. OVs reconstructed at conjugate orders are of the same magnitude of charge but of the opposite signs.

It is well known [1,10,12] that single-charged OVs are stable alone. Free-space propagating beams with such OVs keep not only amplitude distribution (that is typically for all Gaussian beams), but also their initial phase structure. Multiple OVs with charges exceeding unity exist at small distances from the point of nucleation only, and break-up into isolated single-charged OVs of the same sign [14]. This is the reason to test a phase structure of LG_0^2 – mode just at the plane optically conjugated with the plane of a CGH.

Experimental arrangement is shown in Fig. 3. Unexpanded laser beam (He-Ne laser, λ = 0.6328 μm, power $P = 50$ mW, divergence $\theta = 2.5 \cdot 10^{-5}$ rad, $w_0 = 0.8$ mm) diffracts at CGH. Zero diffraction order, LG_0^0 – mode, serves as the reference wave. Using the beam-splitter BS_1, this wave is guided into the reference arm of Mach-Zehnder interferometer, and the singular beam (LG_0^{-1} – mode or LG_0^{-2} – mode) is guided into the object arm. Spatial filters SF_1 and SF_2 pass the working beams only.

A mirror mounted on the piezoceramics PM is fed to the source of direct current PS, whose voltage is controlled from zero to 50 V with the step 0,1 V. Thus, we can gradually change an OPD of two interfering beams within a wavelength. It has been found by graduating of the piezo-mirror that changing of OPD by λ corresponds to changing of voltage by 9,5 V and 9 V, respectively, in the cases of coaxial and off-axis interference for interference angle $\alpha \approx 3.9 \cdot 10^{-3}$ rad. Graduating graph of the used piezo-mirror is shown in Fig. 4.

A reference beam reflected by the piezo-mirror impinges upon objective O ($f' = 35$ mm) that forms divergent Gaussian beam with radius of curvature $R_{ref} = 35$ mm. Singular beam reflected by the mirror M_1 impinges upon the lens L that images the grating plane into the observation one with magnification –1. Two beams are mixed at precisely controlled beam splitter BS_2. Rotation of this beam splitter at small angles and moving the mirror M_1 provide performance of both coaxial and off-axis interference. At the observation plane, where the ratio of the radii of curvature of the wave fronts of mixed singular and smooth beams is $R_S / R_{ref} \approx 513$, CCD camera is placed, being fed to the computer.

Coaxial interference of OVs with charges –1 and –2 and a smooth reference wave for controlled change of an OPD δz is shown in Fig. 5, (a)–(e) and (f)–(j), respec-

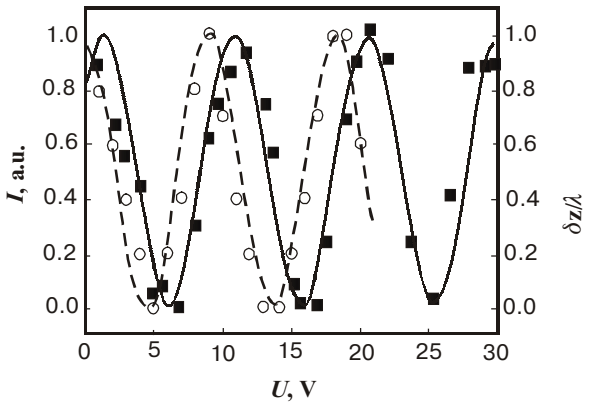

Fig. 4. Behavior of intensity of interference pattern and relative OPD between two beams vs voltage fed to piezo-mirror. The solid and dotted curves correspond to coaxial and off-axis ($\alpha \approx 3.9 \cdot 10^{-3}$ rad $\approx 0.25°$) interference, respectively.

tively. One can see that gradual changing of an OPD results into rotation of the phase maps around the core of OVs with different rate for different charges. As an OPD is changed by a half of a period, then a spiral (projection of a helicoid onto the observation plane) of single-charged OV rotates by 180°, while a spiral associated with two-charged OV rotates only by 90°. The reason is that a pitch of helical phase surface is equal to λ for single-charged OV and to 2λ for two-charged one. One can see also that sub-helicoids of two-charged OV are spaced by λ.

Transition from coaxial interference to off-axis one results in transformation of a spiral to the forklet. In Fig. 6 we show the experimental result of adding of the single-charged singular beam and smooth reference one at the angle ~ $0.8 \cdot 10^{-3}$ rad. Such conditions are close to ones pointed out in Ref. [15], where it has been stated that interference pattern may be regarded as coaxial one up to the angle of interference $0.5 \cdot 10^{-3}$ rad. It can be seen in Fig. 6 (a) "saddle" neighbouring an OV (shown by arrow), and maximum of intensity not far from OV. Changing of the OPD among singular beam and reference one by $\lambda/2$ results in altering of maxima and minima at the interference pattern.

Off-axis interference arrangement is much simpler into adjusting and beam testing, especially when the beam possesses several OVs, which must to be tested simultaneously. Such arrangement is proper also for determination of the charge of OV, equality or difference of the signs of adjacent OVs, or distinct actually singular point (line) from a point (line) of small but non vanishing amplitude. Changing the angle of interference (and, consequently period of interference pattern), one easily distincts m close single-charged OVs from one m-charged OV. Changing of an OPD by δz within λ results in transformations of an interference forklet as it has been mentioned above. The results of computer simulation [10] on transformation of off-axis interference pattern for single-charged OV are compared in Fig. 7 (a) to (d) with the

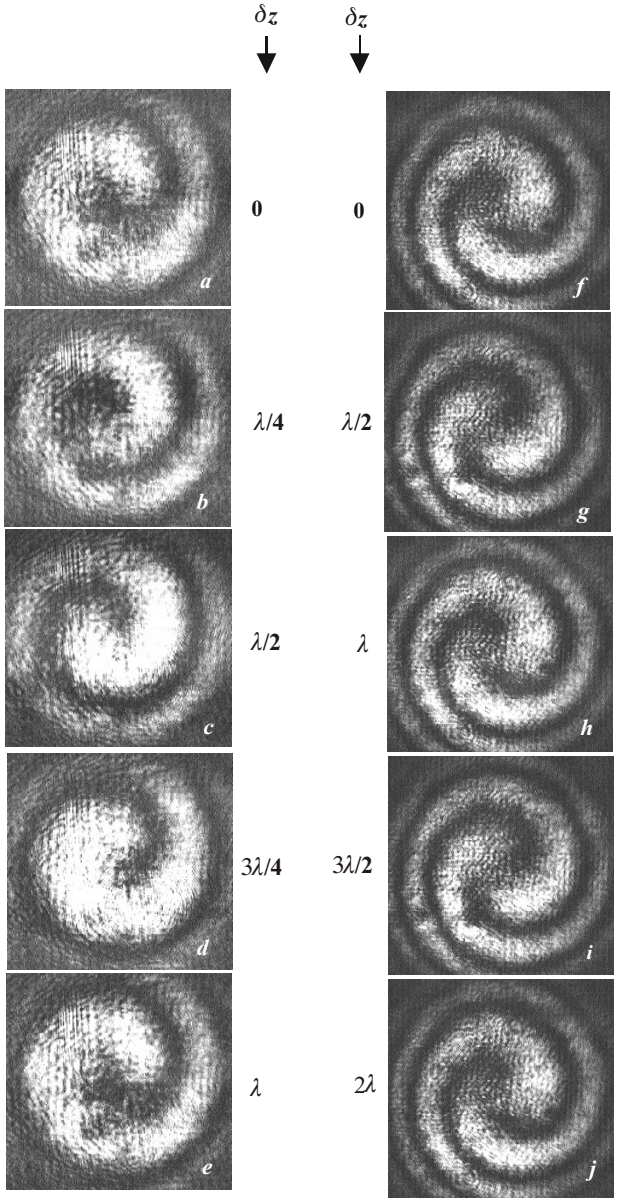

Fig. 5. Testing of OV phase helicoid via coaxial interference with reference Gaussian beams by gradually changed OPD, δz. *a–e* – LG_0^{-1}-mode, $m = -1$, helicoid pitch $\Delta z = l$; *f–j* – LG_0^{-2}-mode, $m = -2$, helicoid pitch $\Delta z = 2l$.

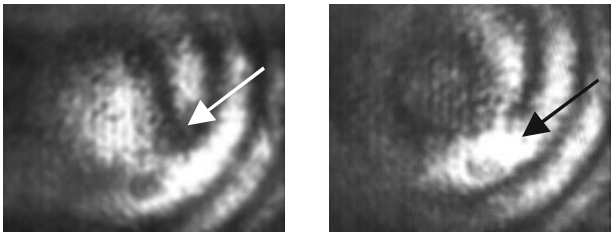

Fig. 6. Interference of vortex beam with the charge $m = -1$ and reference beam demonstrating transition from the spiral structure to the fork-like one; the interference angle $\alpha \approx 0.8 \cdot 10^{-3}$ rad.

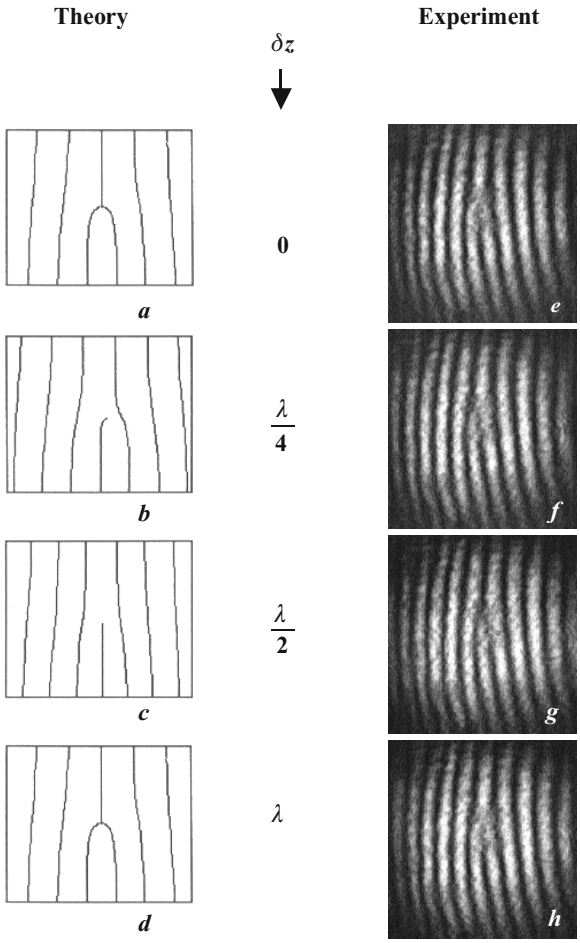

Fig. 7. Testing OV (m = –1) phase helical structure by the off-axial two-beam interference with the reference Gaussian beam.

experimental data (e) to (h), respectively. Dark lines at Fig. 7 (a)–(d) correspond to maxima of the interference pattern.

One can check perfect correspondence of the experimental results with theoretical predictions.

4. Conclusion

Thus, we have demonstrated the possibilities for direct interference detection and testing of 3D helical phase structure of OV. We have verified experimentally the results of computer simulation concerning to transformations of coaxial and off-axis interference patterns produced by OV and a reference wave with smooth wave front due to controlled changing of the OPD within the wavelength. Transition from spiral structure to fork-like one due to changing of interference angle has been observed.

Coaxial interference arrangement is convenient for diagnostics of isolated OVs and provides direct determination both the magnitude and the sign of the OV's topological charge, as well as the radius of curvature of a vortex beam. Resolving power of coaxial technique is mainly dependent on the ratio of radii of curvature of interfering beams. Off-axis interference arrangement is preferable for testing of complex optical fields bearing the set of OV. Resolving power of off-axis technique is determined by the interference angle between superimposed beams.

References

1. J.F. Nye and M.V. Berry, Dislocations in wave trains // *Proc. Roy. Soc. London A* 336, pp.165-190 (1974).
2. J.F. Nye, *Natural focusing and fine structure of light: Caustics and Wave Dislocations*, Institute of Physics Publishing, Bristol (1999).
3. M.S. Soskin, M.V. Vasnetsov, in *Progress in Optics* 42, ed. E. Wolf, pp.219-276, Elsevier, Amsterdam (2001).
4. A.E. Siegman, *Laser*, Chapt.16, University Science Books, Mill Valley, CA (1986).
5. N.B. Baranova, A.V. Mamaev, N.F. Pilipetskii, V.V. Shkunov and B.Ya. Zel′dovich, Wavefront dislocations: topological limitations for adaptive systems with phase conjugation // *J. Opt. Soc. Am.* 73, pp.525-528 (1983).
6. M.W. Beijersbergen, L. Allen, H.E.L.O. van der Ween and J.P. Woerdman, Astigmatic laser mode converters and transfer of orbital angular momentum // *Opt. Comm.* 96, pp.123-132 (1993).
7. A. Nesci, R. Dändliker, M.Salt and H.P.Herzig, Measuring amplitude and phase distribution of fields generated by gratings with sub-wavelength resolution // *Opt.Comm.* 205, pp.229-238 (2002).
8. V.Yu. Bazhenov, M.V. Vasnetsov and M.S. Soskin, Laser beams with screw dislocations of wave front // *Sov. JETP Lett.* 52, pp.429-431 (1990).
9. V.Yu. Bazhenov, M.V. Vasnetsov and M.S. Soskin, Screw dislocations of wavefront // *J.Mod.Optics* 39, pp.985-990 (1992).
10. I.V. Basistiy, M.S. Soskin, M.V. Vasnetsov, Optical wavefront dislocations and their properties // *Opt. Comm.* 119, pp.604-612 (1995).
11. M. Born and E. Wolf, *Principles of Optics*, Pergamon Press, New York (1999).
12. I. Freund, N. Shvartsman and V. Freilikher, Optical dislocation networks in highly random media // *Opt. Comm.* 101, pp. 247-264 (1993).
13. N.R. Heckenberg, R. McDuff, C.P. Smith, and A.G. White, Generation of optical phase singularities by computer-generated holograms // *Optics Lett.* 17, pp.221-223 (1992).
14. I.G. Marienko, M.S. Soskin, M.V. Vasnetsov, Phase reversal of laser beams carrying optical vortices // *Asian Journal of Physics.* 7, N. 3, pp.495-501 (1998).
15. *Optical vortices* (*Horizons in World Physics* 228), Eds. M. Vasnetsov and K. Staliunas, Nova Science Publishers, Inc., NY (1999).